ABCB6 resides in melanosomes and regulates early steps of melanogenesis required for PMEL amyloid matrix formation.

Ptissam Bergam[1,2,3], Johannes M. Reisecker[4], Zsófia Rakvács[5], Nóra Kucsma[5], Graça Raposo[1,2,3], Gergely Szakacs[4,5,*], Guillaume van Niel [1,2,3,6*]

[1] Institut Curie, PSL Research University, UMR144, Centre de Recherche, 26 rue d'Ulm 75231 Paris, France

[2] Centre National de la Recherche Scientifique, UMR144, Paris F-75248, France

[3] Cell and Tissue Imaging Core Facility PICT-IBiSA, Institut Curie.

[4]Institute of Cancer Research, Medical University Vienna, Vienna, Austria

[5]Institute of Enzymology, Research Centre for National Sciences, HAS, Budapest, 1117, Hungary

[6] Center for Psychiatry and Neuroscience, Hopital Saint-Anne, Université Descartes, INSERM U894, Paris, France

[*]Both authors contributed equally to this work.

Correspondance to guillaume.van-niel@inserm.fr and gergely.szakacs@meduniwien.ac.at

Abstract

Genetically inheritable pigmentation defects provide a unique opportunity to reveal the function of proteins contributing to melanogenesis. Dyschromatosis universalis hereditaria (DUH) is a rare pigmentary genodermatosis associated with mutations in the *ABCB6* gene. Here we use optical and electron microscopy imaging combined with biochemical tools to investigate the localization and function of ABCB6 in pigment cells. We show that ABCB6 localizes to the membrane of early melanosomes and lysosomes of the human melanocytic cell line MNT-1. Depletion of ABCB6 by siRNA impaired PMEL amyloidogenesis in early melanosomes and induced aberrant accumulation of multilamellar aggregates in pigmented melanosomes. PMEL fibril formation and normal maturation of pigmented melanosomes could be restored by the overexpression of wild-type ABCB6 but not by variants containing an inactivating catalytic mutation (K629M) or the G579E DUH mutation. In line with the impairment of PMEL matrix formation in the absence of ABCB6, morphological analysis of the retinal pigment epithelium of *ABCB6* knockout mice revealed a significant decrease of melanosome numbers. Our study extends the localization of ABCB6 to melanosomes, suggesting a potential link between the function of ABCB6 and the etiology of DUH to amyloid formation in pigment cells.

Highlights

Mutations of the *ABCB6* gene cause a rare pigmentary defect but its role in pigmentation remains to be clarified.

ABCB6 resides in the early melanosomes and lysosomes of pigment cells.

ABCB6 plays a key role in the early steps of melanogenesis producing PMEL amyloid fibrils.

Our study provides a possible explanation linking ABCB6 mutations to the DUH phenotype.

Keywords

Melanogenesis, ABCB6, ABC transporter, PMEL, amyloid fibrils, melanosomes, pigmentation, trafficking

Abbreviations

PMEL: MELanosomal Protein; TRP-1: Tyrosine Related Protein 1; DUH: Dyschromatosis Universalis Hereditaria; ILV: IntraLuminal Vesicles; ABCB6: ABC transporter B6; RPE: Retinal Pigment Epithelium; APP: Amyloid Precursor Protein; BACE2: Beta-site App-Cleaving Enzyme 2; RCAS1: Receptor-binding Cancer Antigen expressed On Siso cells 1.

Introduction

Hereditary pigmentation defects are caused by mutations in genes that code for key factors involved in melanocyte-specific but also ubiquitous pathways. Each genetic pigmentation disorder offers new clues to the understanding of the pigmentation process encompassing as diverse mechanisms as the generation of melanosomes, melanin synthesis, the transfer of melanin to the keratinocytes or the survival of melanocytes. More than 127 loci are known to affect pigmentation in mouse[1] but the function of the gene products or their implication in pigmentation is only partially understood. Morphological and biochemical studies that revealed mechanisms orchestrating the formation and trafficking of melanosomes have shed light on essential processes whose alterations result in general pigmentation defects[2].

Dyschromatosis universalis hereditaria (DUH) is a pigmentary genodermatosis characterized by a mixture of hyper- and hypo-pigmented macules distributed over the body. The only causative gene reported for DUH encodes the *ATP binding cassette (ABC) transporter subfamily member B6* (*ABCB6*)[3–5]. ABC transporters are large membrane-spanning multidomain proteins promoting the ATP-dependent transmembrane transport of a vast array of biological compounds, including drugs, bile acids, peptides, steroids, ions, and phospholipids. The human genome encodes 48 ABC transporters, which have been grouped

into subfamilies labeled A-G. In addition to the well characterized ABCB1 (P-glycoprotein), responsible for the multidrug resistance phenotype of cancer cells,[6] the ABCB subfamily contains seven half transporters, including the mitochondrial ABC transporters ABCB7, 8 and 10. *ABCB6* is expressed in various cell types including hepatocytes, reticulocytes[7] and pigment cells such as skin melanocytes and the retinal pigment epithelium (RPE)[8]. In erythrocytes, ABCB6 was shown to form the molecular basis of a rare blood group system Langereis (Lan)[7,9]. Interestingly, Lan-negative individuals[7] and mice lacking *ABCB6* are normal, devoid of any pigmentation phenotype[10,11].

ABCB6 was first localized to the outer membrane of mitochondria[12]. Later, several studies suggested extramitochondrial localizations including the plasma membrane[13] or the endolysosomal compartment[14,15,16,17.] Considering the link of *ABCB6* to DUH, this latter localization is of particular interest, because melanosomes are lysosome-related organelles (LRO) of endosomal origin[1,5]. Melanosome biogenesis proceeds through two independent steps. The first step is initiated in a compartment corresponding to early endosomes (stage I melanosomes), where the premelanosomal protein PMEL is processed into amyloid fibrils forming the intraluminal matrix of stage II melanosomes[18]. The formation of PMEL fibrils is dependent on the correct trafficking of PMEL to stage I melanosomes,[19,20] where PMEL is cleaved by several proteases to release luminal amyloidogenic fragments[21–23]. These fragments are sorted onto intraluminal vesicles that are thought to act as nucleating platforms orchestrating mature PMEL fibril formation[24,25]. Interestingly, PMEL fibrils adopt a typical amyloid-like structure and the mechanisms involved in PMEL fibril formation are analogous to the Amyloid Precursor Protein derived pathological amyloid fibril formation in Alzheimer disease. PMEL-derived amyloid structures belong to the emerging category of physiological amyloids that have beneficial cellular functions[18]. Once formed, amyloid fibrils provide a template for the synthesis and storage of eumelanin pigment in later melanosomal stages (stage III and IV, referred here as pigmented melanosomes)[2,7,8]. Mutations affecting PMEL trafficking or processing can be associated with melanin defects [22,26,27]. In such cases, hypopigmentation can result from the generation of cytotoxic amyloid PMEL fragments affecting melanocyte survival or from the reduced stability and/or secretion of pigmented melanosomes[18]. However, studies have also shown that PMEL fibril formation and melanin synthesis can be independent. For example, melanocytes devoid of *PMEL* expression still have normal pigment levels[28] and altered PMEL fibrillation in absence of *ApoE* expression does not affect later stage of melanogenesis[25].

Whereas melanosomes and lysosomes are distinct organelles in melanocytes,[20] recent studies have proposed that lysosomes are required for correct PMEL amyloid matrix formation[29–31],

suggesting a potential role for lysosomal proteins such as ABCB6 in early steps of melanosome biogenesis. Although mutations of the *ABCB6* gene have been linked to a variety of pathophysiological conditions ranging from ocular coloboma to porphyria[32,33], its precise cellular localization and function is not understood. At present, it is unknown if the reported mitochondrial localization of ABCB6 is dependent on specific conditions and cell types related to porphyrin synthesis. Furthermore, the physiological function of ABCB6 in the endo-lysosomal continuum remains to be clarified. In an attempt to understand the link between *ABCB6* mutations and the DUH phenotype, we investigated the subcellular localization and function of ABCB6 in a human melanocytic cell line, MNT-1[20,34]. Our results unequivocally show that ABCB6 resides in the lysosomes and early melanosomes of MNT-1 cells. Ultrastructural analysis of MNT-1 cells depleted for ABCB6 or expressing mutant *ABCB6* variants suggests that ABCB6 regulates early steps of melanosome biogenesis required for the generation of PMEL amyloid fibrils.

Results

ABCB6 localizes to early melanosomes and lysosomes in the human melanocytic cell line MNT1

To assess the localization of ABCB6 in pigment cells, we turned to the widely used human melanocytic cell line MNT-1, which contains the complete machinery needed for efficient melanogenesis[20]. As a first approach, we probed the total cell lysate and various cellular fractions[21] with antibodies recognizing ABCB6 and organelle marker proteins. The ABCB6 signal was present in the cell lysate, and in particular in the light material fraction containing early melanosomes and other endo-lysosomal compartments[21]. Albeit to a lesser extent, ABCB6 was also associated with the dense material fraction containing pigmented melanosomes, but it was completely absent from exosomes and the detergent insoluble fraction that contains only PMEL-derived amyloid fibrils[21]. Taken together, these results suggest that ABCB6 co-fractionates with melanosomes, especially early melanosomes, and does not appear in exosomes that correspond to the secreted intraluminal vesicles from endosomes[25,35] (**Fig 1A**). Immunocytochemical analysis of MNT1 cells by confocal microscopy showed the absence of ABCB6 in mitochondria (labeled by AIF) or the ER (labeled for Calnexin) or the Golgi (labeled by RCAS1) (**Fig 1B**). Further analysis confirmed that the endogenous ABCB6 protein co-localizes primarily with the lysosomal compartments (labeled by LAMP1), and in particular with early (stage II) melanosomes (labeled with Nki-beteb and HMB45). Interestingly, very early melanosomes, labeled with EEA1, and mature (pigmented) melanosomes positive for the

tyrosinase related protein 1 (TRP-1) did not contain appreciable ABCB6 levels, suggesting that ABCB6 is specifically associated with early maturing melanosomes containing processed amyloidogenic PMEL domain fragments and PMEL fibrils, recognized by the Nki-beteb and HMB45 antibodies[36,20] (**Fig 1B,C**). The intracellular localization of the endogenous ABCB6 protein was refined by immunogold labeling of ultrathin cryosections of MNT-1 cells. Electron microscopy pictures showed a clear enrichment of ABCB6 in early maturing melanosomes containing Nki-beteb-labeled material likely corresponding to fibrils, but also its localization in tubulo-vesicular structures containing dense material that we identified as lysosomes (**Fig 1D-E**). Interestingly, ABCB6 was present on the limiting membrane of early melanosomes, in line with its absence on intraluminal vesicles destined to be secreted as exosomes (**Fig 1A**). Thus, these three different methods yielded congruent results, indicating that in MNT-1 cells, endogenous ABCB6 is localized to lysosomes and early melanosomes. This expression pattern is exactly at the crossroad between the endo-lysosomal and the melanosome biogenesis pathways where PMEL fibril formation is initiated[2].

Downregulation of ABCB6 by siRNA perturbs early steps of PMEL amyloid formation without eliminating melanogenesis

To characterize the functional relevance of ABCB6 in melanogenesis, we tested the effect of 6 different siRNA constructs on the expression of endogenous ABCB6 protein and the melanin content of the cells. While ABCB6 depletion did not affect significantly melanin content (**Fig 2A-B**), the individual siRNA constructs induced highly variable changes in cellular melanin contents (**Fig S1A-B**), suggesting that the melanogenesis pathway might have been disturbed. We next investigated trafficking of melanosomal proteins into their respective melanosomal compartments, which is a crucial task during melanogenesis. During normal melanosomal maturation, PMEL is targeted to early melanosomes where it generates amyloid fibrils. Further maturation of melanosomes includes targeting of TRP-1 and other melanogenic enzymes to late stage melanosomes, allowing the production and accumulation of melanin that masks the PMEL epitopes in late stage melanosomes. Immunofluorescence assays using confocal microscopy revealed that, despite efficient depletion of ABCB6 (**Fig 2A**, **Fig S1A)**, both proteins were properly targeted to distinct compartments as in the control situation, indicating proper trafficking of melanosomal proteins and the intact maturation of melanosomes (**Fig 2C**). Localization in lysosomes and early melanosomes indicates that ABCB6 may influence initial steps of melanosome biogenesis [27,37]. We therefore looked for possible defects in the proteolytic processing of PMEL, which have been associated with altered pigmentation[22,28]. Formation of

PMEL-derived fibrils requires the sequential processing of PMEL[22,18]. Using an antibody raised against the cytoplasmic tail of PMEL (PMEL-Cter), we followed the levels of the unglycosylated, full length form of PMEL (P1); the transmembrane M-beta fragment resulting from the first cleavage of P1 by proprotein convertase (MBeta)[21,38]; and the membrane-associated C-terminal fragment (CTF) generated by the processing of the M-beta fragment by the beta-site APP-cleaving enzyme 2 (BACE2) [27]. PMEL CTF is further processed by the gamma-secretase complex containing presenillin-2 in the lysosomes of pigment cells[39]. Importantly, BACE2-mediated cleavage releases the M-alpha fragment, the amyloidogenic luminal domain of PMEL, into the melanosome lumen[27]. The M-alpha fragment is proteolytically processed to produce the amyloidogenic peptides that finally assemble into detergent insoluble protofibrils and fibrils recognized by the HMB45 and I51 antibodies [38].

While the steady state levels of the unglycosylated, full length form of PMEL did not change, downregulation of ABCB6 resulted in an increase of M-beta and CTF levels, suggesting that ABCB6 depletion hinders global PMEL processing without specifically inhibiting any of the cleavage steps (**Fig 2D, Fig S1C**)[1]. We investigated further processing of the luminal amyloidogenic fragments of PMEL by probing the detergent insoluble fraction of MNT-1 cells with HMB45 and I51 antibodies[27,25]. Depletion of ABCB6 by 6 different siRNA constructs (all resulting in the effective downregulation of ABCB6 levels) induced a variable decrease of the steady state levels of PMEL amyloid peptides (**Fig 2E and Fig S1D and E**). This suggested that depletion of ABCB6 may impair the generation of amyloidogenic fragments or affect their fibrillation leading to the generation of aberrant aggregates of PMEL fragments that were not retrieved by classical SDS-PAGE Western-blot analysis.

Electron microscopy (EM) allows the ultrastructural analysis of PMEL amyloid matrix formation. Ultrathin sections of resin embedded MNT-1 cells revealed that depletion of ABCB6 did not change the global ratio between pigmented and unpigmented melanosomes or the number of lysosomes **(Fig 2 F,G)**. However, loss of ABCB6 resulted in a significant decrease in the number of early melanosomes displaying normal PMEL fibril formation **(Fig 2F-G)** and the striking presence of large aggregates filling the lumen of early and late melanosomes (identified by the presence of clathrin coats and melanized fibrils, respectively) **(Fig 2F inset)).** To our knowledge, similar structures have never been reported in melanosomes. The aggregates are reminiscent of EM structures observed in lysosomal storage disorders such as ceroid lipofuscinosis[40], with a more complex, hydrangea-like structure suggestive of lipid-protein complexes. Thus, the EM images confirmed that PMEL fibril formation is altered in absence of ABCB6, leading to the formation of aberrant aggregates in the lumen of early melanosomes.

Such aggregates, once formed in early melanosomes, likely persist and accumulate during their maturation into pigmented melanosomes.

ABCB6 mutations prevent the rescue of normal amyloid fibril formation

To study the potential of ABCB6 to rescue the above described ultrastructural phenotype, we stably transfected MNT-1 cells with constructs encoding either wild-type (WT), an inactive (K629M)[17,41] or a DUH mutant (G579E) *ABCB6* variant[42]. Localization of WT, K629M or G579E ABCB6 was assessed by immunofluorescence confocal microscopy (**Fig3A**). Overall, the exogenously expressed ABCB6 variants displayed a similar localization pattern as the endogenous ABCB6 protein, although the association of the DUH mutant variant with markers of the amyloidogenic luminal domain of PMEL and the PMEL fibrils was less pronounced (**Fig3B**). At the same time, cells expressing the DUH mutant variant displayed a different staining pattern for HMB45 and Nki-beteb suggesting that PMEL luminal fragments were produced but their aggregation into fibrils might have been affected (**Fig3A**).

Next, parental MNT-1 cells, as well as MNT-1 cells stably expressing *ABCB6* variants were depleted for endogenous ABCB6 using an siRNA construct targeting a non-coding region of the gene (siABCB6#2). Western blot analysis of MNT-1 cell lysates revealed that efficient targeting of endogenous ABCB6 still allowed the overexpression of the different ABCB6 variants (**Fig 3C**) providing a model system for rescue experiments. Immunofluorescence assays using antibodies against PMEL and TRP-1 revealed normal localization of both proteins (**Fig 3D**), excluding impaired trafficking of PMEL and the melanogenic enzyme TRP-1 to early and late melanosomes, respectively. As observed for ABCB6 depletion, melanin content was not consistently affected (**Fig S1F**).

Ultrathin cryo-sections of MNT-1 cells immunogold labeled for ABCB6 and the PMEL amyloidogenic domain showed a clear enrichment of wild-type ABCB6 in early melanosomes containing Nki-beteb-labeled fibrils, as shown for the endogenous protein (**Fig 4A,** left panel). Morphological analysis of ultrathin sections of resin embedded MNT-1 cells revealed that expression of wild-type ABCB6 restored the number and morphology of stage II melanosomes, suggesting the rescue of PMEL fibril formation (**Fig 4B,** left panel). At the same time, overexpression of wild-type ABCB6 resulted in a significant increase of the number of lyososomes (**Fig 4C**), indicated by the increased presence of typical multilamellar fingerprint structures. Notably, lamellar and multilamellar structures could be also observed in a minor fraction of early and mature melanosomes (**Fig 4B,** left panel inset).

Images obtained with the two mutant *ABCB6* variants were strikingly different. In both cases, a significant accumulation of aberrant early melanosomes and a decrease of pigmented melanosomes was observed. On immunogold labeled ultrathin cryosections, both mutants were localized to PMEL-positive endocytic structures and lysosomes (**Fig 4A,** middle and right panel), confirming that these mutations did not affect intracellular trafficking. In the case of the catalytically inactive *ABCB6* variant (K629M), stage II melanosomes contained unstructured aggregates of various size, staining positive for PMEL luminal domain (**Fig 4A,** middle panel). Ultrathin sections of resin embedded MNT-1 cells overexpressing the K629M mutant confirmed a complete disorganization of PMEL fibrils in these melanosomes (**Fig 4B,** middle panel; **and Fig 4C**). In line with the presence of unstructured PMEL aggregates, the K629M mutant induced the generation and accumulation of aberrant compartments, likely stage II compartments (**Fig 4B,** middle panel **inset**) full of protofibrils or small aggregates unable to form fully mature amyloid fibrils, but devoid of the hydrangea-like structures observed in the siABCB6 condition. The DUH mutant (G579E) was localized in endosomal compartments containing intraluminal vesicles and unstructured aggregates staining positive for the PMEL luminal domain, suggesting perturbed formation of PMEL fibrils and a defect in the maturation of early melanosomes (**Fig 4A,** right panel). Ultrathin sections of resin embedded MNT-1 cells overexpressing the G579E mutant confirmed impaired fibril formation. The DUH mutant displayed an accumulation of aberrant early, and to a less extent late melanosomes, containing intralumenal multilamellar structures, as observed in cells overexpressing WT ABCB6, and hydrangea-like structures, as observed in ABCB6-depleted cells (**Fig 4B,** right panel **inset**). These results clearly show that in contrast to the wild-type protein, the mutant ABCB6 variants were unable to rescue PMEL fibril formation, failing to restore the number of normal early melanosomes depleted by the downregulation of ABCB6, and inducing instead an accumulation of aberrant stage II melanosomes showing signs of improper PMEL fibril formation. Deeper analysis of the electron micrographs allowed us to further investigate molecular mechanisms controlling PMEL fibril formation. Once cleaved, the luminal domain of PMEL is sorted to intraluminal vesicles that are thought to act as amyloid nucleating seeds of PMEL fibrils[24,43]. Ultrathin sections of resin-embedded MNT-1 cells revealed that in all conditions, intraluminal vesicles were still generated in early melanosomes (**Fig 4D** top panels). Immunogold labeling of cryosections of the same cells with an antibody recognizing the PMEL fibril epitope (Nki-beteb) revealed that in all conditions, the luminal domain of PMEL was released in the lumen of the compartment and was still associated with intraluminal vesicles (**Fig 4D,** bottom panels). Taken together, these data clearly show that ABCB6 influences the

aggregation of PMEL amyloidogenic fragments into fibrils but not former steps involved in PMEL fibril formation. Albeit to a different extent, both the depletion and mutation of ABCB6 resulted in the disorganization of PMEL fibrils, preventing normal maturation and organization of the amyloid matrix.

Genetic disruption of Abcb6 results in subtle ultrastructural changes of retinal pigmented epithelium in mice.

Melanogenesis *in vivo* can be morphologically analyzed by conventional electron microscopy (EM) analysis of the retinal pigment epithelium (RPE) of the eyes [25]. To assess the role of ABCB6 in RPE pigmentation, we determined the structure of RPE by examining the retinal ultrastructure of 6-month-old *ABCB6*$^{-/-}$, *ABCB6*$^{-/+}$ and *ABCB6*$^{+/+}$ mice. Compared to the normal ultrastructure of wild type (WT) RPE, the density of melanosomes in the RPE of *ABCB6*$^{+/-}$ and *ABCB6*$^{-/-}$ mice was significantly lower (**Fig 5 A,B**). A similar decrease in melanosome numbers was described in conditions associated with a defect in PMEL fibril formation and the aggregation of aberrant and toxic PMEL amyloidogenic fragments damaging melanosome integrity[26]. However, the shape of melanosomes, expressed as a ratio between width and length, was normal in *ABCB6* knockout mice, contrary to the rounded morphology of melanosomes in mouse strains with impaired PMEL fibril formation [22,44,45] (**Fig 5C**). These results confirmed the in vivo relevance of ABCB6 in melanosome biogenesis in the RPE.

Discussion

Dyschromatosis Universalis Hereditaria (DUH) is a rare autosomal dominant genodermatosis characterized by asymptomatic hyper- and hypo-pigmented macules that appear in infancy or early childhood. The etiopathology of DUH is not known. Lesions show a focal increase or decrease in melanin and melanosome content of melanocytes and keratinocytes of the basal layer, which is believed to be the consequence of a defect in melanosome production and/or distribution, rather than a disorder of melanocyte numbers[42,46,47]. Several associated conditions have been reported, including ocular abnormalities, photosensitivity, neurosensory hearing defects, mental retardation and erythrocyte, platelet and tryptophan metabolism abnormalities[48]. Although the role of environmental factors cannot be excluded, at present it is not clear if these conditions represent a single disease entity, especially because DUH patients with ABCB6 mutations do not exhibit any of the additional abnormalities.

The pigmentation defect of DUH patients led us to investigate the role of ABCB6 in melanogenesis. We are far from attributing each melanosomal protein with a defined function

in melanogenesis or melanosome secretion. However, proteins implicated in hereditary pigmentation defects often reveal key mechanisms. In this study, we used the MNT-1 cell line as a pigment cell model to characterize the role of ABCB6 in melanogenesis. MNT-1 is a highly pigmented human melanoma cell line that is widely used as a model system as it has conserved the complete machinery to continuously produce all melanosome stages, from the generation of PMEL amyloid fibrils to the synthesis of eumelanin[2,20]. Several reports have used this cell line for localization studies and to reveal the role of key proteins involved in intracellular trafficking[2749], proteolytic cleavage[22] and signaling pathways[50] regulating melanogenesis.

Using complementary methods, we show that the endogenous ABCB6 protein is localized to the lysosomes and early melanosomes of MNT-1 cells. Our results confirm previous localization of ABCB6 in the endolysosomal continuum [16,17] and indicate that ABCB6 does not localize to the mitochondria of MNT-1 cells. Several ABC transporters have been associated with melanocytes and melanoma cells[51,52], and mass spectrometry analysis already suggested the presence of ABCB6 in purified early melanosomes [53], but to our knowledge, this is the first study to unequivocally demonstrate the presence of an ABC transporter in the membrane of melanosomes. While ABCB6 is present on exosomes of reticulocytes [16], it was not observed in the exosome fraction of MNT-1 cells, in line with known differences in the sorting mechanisms of melanocytes and reticulocytes[35].

Melanosomes and lysosomes are distinct compartments in MNT-1 cells[20], although lysosomes are thought to contribute to PMEL CTF processing[39] and to PMEL fibril formation during early melanogenesis[29–31] by a yet unknown mechanism. In a first attempt to understand the role of ABCB6 in melanogenesis, we depleted ABCB6 by siRNA in MNT-1 cells. Overall melanin levels, the sorting of melanosomal proteins, the formation of intraluminal vesicles appeared normal, but the cleavage of the full length PMEL was slightly affected and the apparent steady state levels of PMEL amyloidogenic fragments were significantly decreased (Fig 2 D, E). Modulation of amyloidogenic PMEL fragment levels can result from a defect of PMEL cleavage[22], PMEL sorting[27], an inhibition of lysosomal protease activity[39], or the loss of melanosomal identity[44]. In all these conditions, the decrease of amyloidogenic PMEL fragment levels was associated with disturbed PMEL fibril formation. Strikingly, morphological analysis at the ultrastructural level revealed the appearance of large aggregates displaying a hydrangea-like morphology in early and mature melanosomes of cells depleted for ABCB6 or expressing ABCB6 mutants. Based on their morphology, the aberrant structures are likely composed of proteo-lipid aggregates, corresponding to the unstructured aggregates containing PMEL luminal domain, as observed in cryosections of cells embedded in gelatin for immunogold

labeling. We interpret these results to suggest that defects of ABCB6 levels and/or function result in the impaired assembly of PMEL amyloidogenic fragments into well-organized fibrils. Ultimately, impaired assembly leads to aberrant aggregates that could not be detected by SDS-PAGE and Western blotting, explaining the apparent decrease of steady state levels of PMEL amyloidogenic fragments, but that were clearly visible on the EM images. Deeper biochemical investigations are required to characterize the composition of the aggregates, which could reveal the molecular basis of the pathological PMEL aggregation.

The clear defect in amyloid formation observed in ABCB6-depleted MNT-1 cells is at odds with the normal phenotype of the *ABCB6* knockout mice and the lack of pigmentation abnormalities in Lan-negative individuals[54]. Normal melanogenesis may be explained by compensatory mechanisms, or in the case of knockout mice the lack of external stress factors in the well-controlled laboratory environment, where the function of the ABC transporter-based "chemoimmunity network" responsible for detoxification may be less relevant[55]. Importantly, in contrast to human skin, mice skin does not contain melanocytes, which are only present in hair follicles[56]. Therefore, the effect of ABCB6 depletion in the human melanocyte model MNT-1 may not be relevant for mice pigmentation. Here we show that beneath the normal fur of *ABCB6* $^{-/-}$ mice, there are subtle but significant differences in the ultrastructure of the retinal pigment epithelium, where formation of melanosomes is restricted to a brief developmental period[57]. We attribute the decrease of melanosome density in the RPE of *ABCB6* $^{+/-}$ and $^{-/-}$ mice to an early defect in melanosomal biogenesis that would impair their formation or integrity. Similar phenotypes were described in conditions associated with a defect in PMEL fibril formation and the aggregation of aberrant and toxic PMEL amyloidogenic fragments damaging melanosome integrity[26]. However, unlike conditions where PMEL fibril formation was completely impaired [22,44,45,] the shape of the remaining melanosomes in the RPE of *ABCB6* knockout mice was not abnormal.

Using an siRNA construct targeting a non-coding region and the lentiviral system to downregulate and overexpress ABCB6, respectively, we were able to study the potential of ABCB6 variants to rescue MNT1 cells from the ABCB6-depletion phenotype. We show that rescue with the wild-type form of ABCB6 almost fully restores the generation of PMEL fibrils, although it also increased the generation of multilamellar lysosomal structures. Mutation of the catalytic Walker A lysine residue is known to impair the function of ABC transporters[58], and several DUH mutations are predicted to be deleterious – including the G579E mutation, which affects a non-conserved amino acid in the cytoplasmic nucleotide binding domain[59]. Contrary to former reports showing accumulation in the Golgi[4], ABCB6 G579E was properly targeted

to melanosomes. Since neither the K629M nor the G579E mutant ABCB6 variant was able to restore normal biogenesis of PMEL fibrils and both induced the accumulation of unpigmented aberrant melanosomes, we believe it is likely that the G579E mutation impairs the function of ABCB6. Considering the dominant inheritance of DUH and the homodimerisation of ABCB6[16,60], a straightforward explanation is that DUH mutations antagonize the wild-type allele through a dominant negative effect.

How can a defect of PMEL matrix formation lead to the complex pigmentation changes observed in DUH patients? The localization of ABCB6 in early melanosomes, the variable modulation of melanin levels by anti-ABCB6 siRNA and the morphological changes observed by electron microscopy all point toward a defect in early melanogenesis involving PMEL amyloid fibril formation. Subtle defects in PMEL fibril formation are known to result in altered melanin deposition, affecting the integrity of mature melanosomes and ultimately leading to variable changes in global melanin concentrations[22,26,28]. Similarly to the *ABCB6*-null phenotype, complete depletion of PMEL has only a subtle effect on the coat color of mice[28], while silver mice expressing a truncated version of PMEL are unable to produce a functional matrix[26], and BACE2 knock out mice that fail to process PMEL[22] display a grey coat color. The hypopigmented areas characteristic to DUH may result from a defect in the maturation of early melanosomes or from the compromised integrity of pigmented melanosomes due to the accumulation of PMEL toxic oligomers[36].

The DUH mutation results in the accumulation of the amyloid PMEL luminal domain in multivesicular compartments, and loss of ABCB6 induces the accumulation of hydrangea-like structures. Based on these results we hypothesize that ABCB6 regulates critical steps in the formation of the PMEL matrix. However, the DUH mutation did not abolish processing of PMEL, nor the sorting of its luminal domain onto intraluminal vesicles (Fig 4D). Rather, the defect seems to be associated with the last steps of fibrillation where the amyloidogenic PMEL fragments turn into mature fibrils on the surface of intraluminal vesicles[24]. Similarly, the major defect in ABCB6-depleted cells is associated with the aberrant aggregation of amyloid PMEL luminal domains on the surface of intraluminal vesicles. Based on these observations it is tempting to speculate that the function of ABCB6 is required for maintaining the intraluminal homeostasis of the maturing early melanosome, which is needed for efficient fibrillation and matrix formation.

The ABCB6-related morphological alterations also raise the possibility that the observed phenotype is due to an indirect effect, mediated by lysosomes, which are thought to contribute to early melanosome biogenesis and the control of the fibrillation of PMEL amyloidogenic

domains[29–31]. Given the increased number of lysosomes and the presence of lysosomal structures in the melanosomes of cells overexpressing wild-type ABCB6 or the G579E mutant, it is tempting to speculate that ABCB6 may regulate lysosome-related processes. Lysosomal proteases have been reported to process different fragments of PMEL during early steps of melanogenesis[29–31,39]. Thus, ABCB6 may either regulate lysosome activity or support potential inter-organelle interactions between lysosomes and early melanosomes that remain to be demonstrated. Finally, we cannot exclude the possibility that the DUH phenotype is due to a defect in the transfer of mature melanosomes to keratinocytes- this hypothesis will need testing in a different experimental setup, as pigmentation of the fur coat is not an appropriate model for melanosome transfer[56]. Once transferred to keratinocytes, melanosomes are either stored in non-degradative compartments[61,62] or are degraded by lysosomal hydrolases[37,63]. It is also possible that ABCB6 influences these events through its expression and function in lysosomes of keratinocytes. A role in early melanogenesis in melanocytes and melanosome storage/degradation in keratinocytes are not mutually exclusive, and may explain the morphology of DUH skin biopsies, which indicated a normal number of intact melanocytes in both the hypo- and hyper-pigmented skin areas[42], a lower number of mature melanosomes in hypo-pigmented macules and an accumulation of pigmented melanosomes in melanocytes and in keratinocytes in hyper-pigmented macules.

In summary, our study shows that *ABCB6* is expressed in lysosomes and early melanosomes of pigment cells and regulate early steps of melanogenesis. Understanding the relevance of ABCB6 in melanogenesis will require a better understanding of the function of ABCB6 in the endolysosomal system. Ongoing work in our laboratories focuses on the role of ABCB6 in the formation of PMEL amyloid fibrils under normal or pathologic conditions.

Glossary

Pigmentation: All processes related to the acquisition or generation of pigment, notably melanin.

Melanin: pigments (from yellow to black) that are produced by melanocytes and retinal pigment epithelium among other cell types.

Melanosomes: intracellular compartment of pigment cells, also called lysosome-related organelles.

Functional Amyloid: protein or peptides that adopt or display a beta-sheet enriched structures and forms insoluble organized structures, often as fibrils. Contrary to pathological amyloids, they serve physiological purpose.

ABC (ATP-Binding Cassette) transporters: A superfamily of carrier proteins containing two highly conserved ATP-binding cassettes, promoting the active transmembrane transport of a large array of molecules.

Acknowledgements

We thank Dr. James Gallo (Mount Sinai School of Medicine) for the permission to use cryopreserved Abcb6 -/- mouse sperm. We thank the PITC-IBiSA Imaging Facility, the Institut Curie (Paris), the Nikon Imaging Center and the members of the France-BioImaging national research infrastructure for assistance with microscopy. This work was supported by Institut Curie, CNRS, by the Fondation ARC pour la Recherche sur le Cancer (grant SL220100601359) (to GR), by the Fondation pour la Recherche Médicale (AJE20160635884) (to GvN), by a Research Grant from the Amyloidosis Foundation (to GvN). GS was supported by a Momentum grant of the Hungarian Academy of Sciences. Funding from the Austrian Science Fund (SFB35, GS) is also acknowledged.

Figure Legends:

Figure 1. Subcellular localization of the endogenous ABCB6 protein in MNT-1 cells.

A. Total cellular lysates, the insoluble fraction (Pmel fibrils), light material fraction (LMF, early melanosomes), dense material fraction (DMF, mature melanosomes) and the exosomes were isolated from MNT-1 cells as described in the Materials and methods section. Cellular fractions were analysed by Western-blotting using antibodies raised against specific markers of exosomes (Alix), PMEL fibrils (HMB45) mature melanosomes (TRP-1), and ABCB6. Tubulin is shown as a loading control.

B. Determination of the subcellular localization of ABCB6 by immunofluorescence labelling and laser-scanning confocal microscopy. Expression of the endogenous ABCB6 protein in MNT-1 cells was visualized by the OSK43 ABCB6 antibody (green); nuclei were labelled with Hoechst 33342 (blue); organelles were labelled with specific markers (red): ER (Calnexin), Golgi (RCAS1), mitochondria (AIF), early endosomes (EEA1), lysosomes (LAMP1). Non-pigmented melanosomes were labelled using an antibody directed against the luminal domain

of PMEL (Nki-bteb) and HMB45; pigmented melanosomes were stained with TRP-1. Scale bar: 10μm.

C. Pearson's correlation coefficients for colocalization of ABCB6 with organelle-specific markers shown in B.

D. Top and bottom panels. Ultrathin cryosections of MNT-1 cells were double immunogold labelled for PMEL luminal domain (Nki-beteb, PAG 10nm) and ABCB6 (PAG 15nm). Arrows indicate colocalization of endogenous ABCB6 and PMEL in non-pigmented melanosomes; asterisks show ABCB6 in lysosomal tubulovesicular structures. Mitochondria are annotated with "m". Scale bar, 500 nm.

E. Quantification of immunogold labelling of endogenous ABCB6 in MNT-1 cells. Gold particles representing labelling for ABCB6 in the EM analysis were counted and assigned to the indicated compartments, which were identified based on morphology. Data are presented as the mean percentage of total gold particles in each compartment.

Figure 2. Effect of ABCB6 depletion on melanogenesis

A. Downregulation of ABCB6 in MNT-1 cells. Western blot analysis of whole cell lysates isolated from MNT-1 cells treated with control or anti-ABCB6 siRNA constructs. Tubulin is shown for loading control.

B. Effect of ABCB6 depletion on the intracellular melanin content of MNT-1 cells. Values show averaged melanin levels obtained after treatment with 6 different siRNA constructs (MNT1 siABCB6), relative to control (siCtrl). See Supplementary Fig. 2B for details.

C. Downregulation of ABCB6 does not influence trafficking of melanosomal proteins. Subcellular localization of melanosomes was followed by confocal microscopy; using antibodies labelling early (Nki-beteb, red) and late melanosomes (TRP-1, green). Nuclei are stained with DAPI (blue).

D. Detergent-soluble lysates of MNT-1 cells treated with control siRNA (siCtrl) or ABCB6 siRNA (siABCB6) analysed by immunoblotting, using antibodies against the PMEL C-terminus (anti-PMEL-C) and tubulin. The different PMEL fragments are annotated on the left.

E. Detergent-insoluble lysates of MNT-1 cells treated with control siRNA (siCtrl) or ABCB6 siRNA (siABCB6) were analysed by immunoblotting using antibodies against PMEL amyloidogenic domains (anti-PMEL-HMB45 and anti-PMEL-I51) and tubulin.

F. Representative ultrathin section images of control and ABCB6 depleted MNT-1 cells embedded in resin. Black arrowheads indicate stage I melanosomes, white arrowheads point to

mature melanosomes containing PMEL fibrils covered by melanin. White arrows point to aberrant melanosomes containing a "hydrangea-like" structure (enlarged in the inset). Scale: 1 μm.

G. Quantification of endosomal/melanosomal compartments, as defined by the morphology of the organelles in conventional EM of control or ABCB6-depleted MNT-1. Values represent the percentage of each compartment relative to all of the endosomal/melanosomal compartments identified in 20 cell profiles per condition. P values: * = $p<0.05$, ** = $p<0.02$, *** = $p<0.01$.

Figure 3. Expression of ABCB6 variants in MNT-1 cells

A. Determination of the subcellular localization of ABCB6 by immunofluorescence labelling and laser-scanning confocal microscopy. Expression of wild-type (ABCB6 WT), and mutant ABCB6 variants (ABCB6 K629M and ABCB6 G579E) was visualized in MNT-1 cells using the OSK ABCB6 antibody (green); nuclei were labelled with Hoechst 33342 (blue); organelles were labelled with specific markers (red): ER (Calnexin), Golgi (RCAS1), mitochondria (AIF), early endosomes (EEA1), lysosomes (LAMP1). Non-pigmented melanosomes were labelled using an antibody directed against the luminal domain of PMEL (Nki-beteb and HMB45); pigmented melanosomes were stained with TRP-1 (red). Scale bar: 10μm.

B. Pearson's correlation coefficients for colocalization of ABCB6 variants with the organelle-specific markers.

C. Western blot analysis of whole cell lysates isolated from parental MNT-1 cells (Parent), MNT-1 cells overexpressing wild-type ABCB6 (ABCB6 WT), a catalytically inactivate form of ABCB6 (ABCB6 K629M) or a DUH mutant variant (ABCB6 G579E). Cells were either treated with control or anti-ABCB6 siRNA (#2) constructs. Tubulin is shown for loading control.

D. Overexpression of ABCB6 variants does not influence trafficking of melanosomal proteins. Subcellular localization of melanosomes was followed by confocal microscopy using antibodies labelling early (Nki-beteb, red) and late melanosomes (TRP-1, green). Nuclei are stained with DAPI (blue).

Figure 4. Overexpression of DUH mutant ABCB6 fails to rescue the ABCB6 depletion phenotype.

A. Ultrathin cryosections of MNT-1 cells overexpressing ABCB6 WT (left panel), inactive ABCB6 (middle panel) or the DUH variant (right panel) were double immunogold labelled for

PMEL luminal domain (PAG 10nm) and ABCB6 (PAG 15nm). Arrowheads indicate colocalization of ABCB6 and PMEL in non-pigmented melanosomes. Mitochondria are annotated with "m". Scale bar, 500 nm.

B. Representative ultrathin section images of resin-embedded control and ABCB6 depleted MNT-1 cells and MNT-1 cells overexpressing wild-type ABCB6 (lower left panel), inactive ABCB6 (lower middle panel) or the DUH variant (lower right panel). Melanosome stages are annotated from I to IV; black flowers indicate aberrant pigmented melanosomes containing unstructured aggregates along with melanised fibers. White stars indicate aberrant lysosomal structures. LD: lipid droplet, V: Vacuole, Lys: Lysosome, M: Mitochondria. Scale bar is 500nm.

C. Quantification of endosomal/melanosomal compartments as defined by the morphology of the organelles in conventional EM of control or ABCB6-depleted MNT-1 with or without the overexpression of wild-type (ABCB6 WT) or mutant ABCB6 variants (ABCB6 K629M, ABCB6 G579E). Values represent the percentage of each compartment relative to all endosomal/melanosomal compartments identified in 20 cell profiles per condition. P values : * = $p<0.05$, ** = $p<0.02$, *** = $p<0.01$

D. Top panel: Ultrathin cryosections of MNT-1 cells treated with (from left to right) control siRNA or anti ABCB6 siRNA; or overexpressing ABCB6 WT, inactive ABCB6, or the DUH variant. Arrows point to intraluminal vesicles in early melanosomes. Scale bar, 200 nm. Bottom panels: MNT-1 cells treated as shown in the top panels were embedded in gelatin to obtain ultrathin cryosections that were double immunogold labelled for PMEL luminal domain (Nki-beteb, PAG 10nm) and a lysosomal lipid (LBPA, PAG 15nm) for siRNA conditions, or for PMEL luminal domain (Nki-beteb, PAG 10nm) and ABCB6 (PAG 15nm) for overexpressing conditions. Arrows indicate the presence of PMEL luminal domain on intraluminal vesicles in early melanosomes. Scale bar, 200 nm.

Figure 5. Electron microscopy analysis of the retinal ultrastructure of Abcb6$^{-/-}$, Abcb6 $^{-/+}$ and Abcb6 $^{+/+}$ mice

A. EM analysis of resin embedded RPE of adult *ABCB6*$^{+/+}$, ABCB6$^{+/-}$ and ABCB6$^{-/-}$ mice (Scale bar: 2µm).

B. Quantification of melanosome number per µm2 of RPE. More than 300 melanosomes were quantified in 10 electron micrographs obtained from 3 independent samples for each condition.

C. Quantification of the ratio (R) of the maximal width and length of melanosomes for each condition. More than 100 melanosomes were measured in 10 electron micrographs obtained from 3 independent samples for each condition.

Supplementary Figures.

A. Quantification of ABCB6 mRNA expression by RT-PCR following treatment of MNT-1 cells with control siRNA control or siRNA against ABCB6.

B. Quantification of intracellular melanin contents of MNT-1 cells after treatment with each ABCB6 siRNA constructs.

C. Quantification of PMEL fragments recognized by anti-PMEL-C antibody in the detergent soluble fraction (based on band intensities shown in Figure 2D).

D. Quantification of PMEL amyloidogenic fragments labelled by the HMB45 antibody in the detergent insoluble fraction after siRNA treatment of MNT1 cells.

E. Quantification of PMEL amyloidogenic fragments labelled by the I51 antibody in the detergent insoluble fraction after siRNA treatment of MNT1 cells.

F. Quantification of intracellular melanin contents of MNT-1 cells after overexpression of ABCB6 variants with or without treatment with ABCB6 siRNA #2.

G. Ultrathin cryosections of MNT-1 cells treated with ABCB6 siRNA that were double immunogold labelled for PMEL luminal domain (Nki-beteb, PAG 10nm) and ABCB6 (PAG 15nm). Absence of ABCB6 labeling after ABCB6 siRNA treatment supports the specificity of the labelling. White arrows indicate aberrant early melanosomes labelled for PMEL and "m" indicates mitochondria. Scale bar, 1 μm.

References

1. Passeron, T., Mantoux, F. & Ortonne, J. P. Genetic disorders of pigmentation. *Clinics in Dermatology* **23,** 56–67 (2005).
2. Raposo, G. & Marks, M. S. Melanosomes — dark organelles enlighten endosomal membrane transport. *Nature* **8,** (2007).
3. Lu, C. *et al.* Novel missense mutations of ABCB6 in two chinese families with dyschromatosis universalis hereditaria. *J. Dermatol. Sci.* **76,** 255–258 (2014).
4. Zhang, C. *et al.* Mutations in ABCB6 Cause Dyschromatosis Universalis Hereditaria. (2013). doi:10.1038/jid.2013.145
5. Liu, H. *et al.* Genome-wide linkage, exome sequencing and functional analyses

identify ABCB6 as the pathogenic gene of dyschromatosis universalis hereditaria. *PLoS One* **9,** e87250 (2014).

6. Szakacs, G., Paterson, J. K., Ludwig, J. A., Booth-Genthe, C. & Gottesman, M. M. Targeting multidrug resistance in cancer. *Nat. Rev. Drug Discov.* **5,** 219–234 (2006).
7. Helias, V. *et al.* ABCB6 is dispensable for erythropoiesis and specifies the new blood group system Langereis. *Nat. Genet.* (2012). doi:10.1038/ng.1069
8. S, H., Ak, B., Langmann, T., Ecker, J. & Schmitz G. Mapping ATP-binding cassette transporter gene expression profiles in melanocytes and melanoma cells. *Melanoma Res* **17,** 265–73 (2007).
9. Koszarska, M. *et al.* Screening the expression of ABCB6 in erythrocytes reveals an unexpectedly high frequency of Lan mutations in healthy individuals. *PLoS One* **9,** e111590 (2014).
10. Chavan, H. *et al.* Functional coupling of ATP-binding cassette transporter Abcb6 to cytochrome P450 expression and activity in liver. *J. Biol. Chem.* **290,** 7871–7886 (2015).
11. Fukuda, Y. *et al.* The severity of hereditary porphyria is modulated by the porphyrin exporter and Lan antigen ABCB6. *Nat. Commun.* **7,** (2016).
12. Krishnamurthy, P. C. *et al.* Identification of a mammalian mitochondrial porphyrin transporter. *Nature* **443,** 586–589 (2006).
13. Paterson, J. K. *et al.* Human ABCB6 localizes to both the outer mitochondrial membrane and the plasma membrane. *Biochemistry* **46,** 9443–9452 (2007).
14. Jalil, Y. A. *et al.* Vesicular localization of the rat ATP-binding cassette half-transporter rAbcb6. *Am. J. Physiol. Cell Physiol.* **294,** C579-590 (2008).
15. Bagshaw, R. D., Mahuran, D. J. & Callahan, J. W. A proteomic analysis of lysosomal integral membrane proteins reveals the diverse composition of the organelle. *Mol Cell Proteomics* **4,** 133–43 (2005).
16. Kiss, K. *et al.* Shifting the paradigm: the putative mitochondrial protein ABCB6 resides in the lysosomes of cells and in the plasma membrane of erythrocytes. *PLoS One* **7,** e37378 (2012).
17. Kiss, K. *et al.* Role of the N-terminal transmembrane domain in the endo-lysosomal targeting and function of the human ABCB6 protein. *Biochem J* **467,** 127–139 (2015).
18. Bissig, C., Rochin, L. & van Niel, G. PMEL Amyloid Fibril Formation: The Bright Steps of Pigmentation. *Int. J. Mol. Sci.* **17,** (2016).
19. Schonthaler, H. B. *et al.* A mutation in the silver gene leads to defects in melanosome

biogenesis and alterations in the visual system in the zebrafish mutant fading vision. *Dev. Biol.* (2005). doi:10.1016/j.ydbio.2005.06.001

20. Raposo, G., Tenza, D., Murphy, D. M., Berson, J. F. & Marks, M. S. Distinct protein sorting and localization to premelanosomes, melanosomes, and lysosomes in pigmented melanocytic cells. *J. Cell Biol.* **152,** 809–823 (2001).
21. Berson, J. F. *et al.* Proprotein convertase cleavage liberates a fibrillogenic fragment of a resident glycoprotein to initiate melanosome biogenesis. *J Cell Biol* **161,** 521–533 (2003).
22. Rochin, L. *et al.* BACE2 processes PMEL to form the melanosome amyloid matrix in pigment cells. *Proc. Natl. Acad. Sci.* **110,** 10658–10663 (2013).
23. van Niel, G. *et al.* The tetraspanin CD63 regulates ESCRT-independent and -dependent endosomal sorting during melanogenesis. *Dev. Cell* **21,** 708–721 (2011).
24. Hurbain, I. *et al.* Electron tomography of early melanosomes: Implications for melanogenesis and the generation of fibrillar amyloid sheets. *Amyloid Int. J. Exp. Clin. Investig.* 26–31 (2008).
25. van Niel, G. *et al.* Apolipoprotein E Regulates Amyloid Formation within Endosomes of Pigment Cells. *Cell Rep.* (2015). doi:10.1016/j.celrep.2015.08.057
26. Watt, B. *et al.* Mutations in or near the transmembrane domain alter PMEL amyloid formation from functional to pathogenic. *PLoS Genet.* **7,** e1002286 (2011).
27. van Niel, G. *et al.* The tetraspanin CD63 regulates ESCRT-independent and -dependent endosomal sorting during melanogenesis. **21,** 708–721 (2011).
28. Hellstrom, A. R. *et al.* Inactivation of Pmel alters melanosome shape but has only a subtle effect on visible pigmentation. *PLoS Genet.* **7,** e1002285 (2011).
29. Ho, T., Watt, B., Spruce, L. A., Seeholzer, S. H. & Marks, M. S. The Kringle-like Domain Facilitates Post-endoplasmic Reticulum Changes to Premelanosome Protein (PMEL) Oligomerization and Disulfide Bond Configuration and Promotes Amyloid Formation. *J Biol Chem* **291,** 3595–3612 (2016).
30. Kawaguchi, M., Hozumi, Y. & Suzuki, T. ADAM protease inhibitors reduce melanogenesis by regulating PMEL17 processing in human melanocytes. *J. Dermatol. Sci.* **78,** 133–142 (2015).
31. Leonhardt, R. M., Vigneron, N., Hee, J. S., Graham, M. & Cresswell, P. Critical residues in the PMEL/Pmel17 N-terminus direct the hierarchical assembly of melanosomal fibrils. *Mol. Biol. Cell* **24,** 964–981 (2013).
32. Wang, L. *et al.* ABCB6 mutations cause ocular coloboma. *Am. J. Hum. Genet.* (2012).

doi:10.1016/j.ajhg.2011.11.026

33. Boswell-Casteel, R. C., Fukuda, Y. & Schuetz, J. D. ABCB6, an ABC Transporter Impacting Drug Response and Disease. *AAPS J.* **20,** 8 (2017).
34. Kushimoto, T. *et al.* A model for melanosome biogenesis based on the purification and analysis of early melanosomes. *Proc Natl Acad Sci U S A* **98,** 10698–10703 (2001).
35. van Niel, G., D'Angelo, G. & Raposo, G. Shedding light on the cell biology of extracellular vesicles. *Nat. Rev. Mol. Cell Biol.* (2018). doi:10.1038/nrm.2017.125
36. Watt, B. *et al.* N-terminal domains elicit formation of functional Pmel17 amyloid fibrils. *J Biol Chem* **284,** 35543–35555 (2009).
37. Diment, S., Eidelman, M., Rodriguez, G. M. & Orlow, S. J. Lysosomal hydrolases are present in melanosomes and are elevated in melanizing cells. *J. Biol. Chem.* **270,** 4213–4215 (1995).
38. Leonhardt, R. M., Vigneron, N., Rahner, C. & Cresswell, P. Proprotein convertases process Pmel17 during secretion. *J Biol Chem* **286,** 9321–9337 (2011).
39. Sannerud, R. *et al.* Restricted Location of PSEN2/gamma-Secretase Determines Substrate Specificity and Generates an Intracellular Abeta Pool. *Cell* **166,** 193–208 (2016).
40. Smith, K. R. *et al.* Cathepsin F mutations cause Type B Kufs disease, an adult-onset neuronal ceroid lipofuscinosis. *Hum. Mol. Genet.* **22,** 1417–1423 (2013).
41. Grebowski, J., Studzian, M., Bartosz, G. & Pulaski, L. Leishmania tarentolae as a host for heterologous expression of functional human ABCB6 transporter. *Biochim. Biophys. Acta - Biomembr.* **1858,** 2617–2624 (2016).
42. Cui, Y. X. *et al.* Novel mutations of ABCB6 associated with autosomal dominant dyschromatosis universalis hereditaria. *PLoS One* **8,** e79808 (2013).
43. van Niel, G. *et al.* Apolipoprotein E Regulates Amyloid Formation within Endosomes of Pigment Cells. *Cell Rep.* (2015). doi:10.1016/j.celrep.2015.08.057
44. Giordano, F., Bonetti, C., Surace, E. M., Marigo, V. & Raposo, G. The ocular albinism type 1 (OA1) G-protein-coupled receptor functions with MART-1 at early stages of melanogenesis to control melanosome identity and composition. *Hum Mol Genet* **18,** 4530–4545 (2009).
45. Brunberg, E. *et al.* A missense mutation in PMEL17 is associated with the Silver coat color in the horse. *BMC Genet.* **7,** (2006).
46. Al Hawsawi, K., Al Aboud, K., Ramesh, V. & Al Aboud, D. Dyschromatosis universalis hereditaria: Report of a case and review of the literature. *Pediatr. Dermatol.*

19, 523–526 (2002).

47. Kim, N. S., Im, S. & Kim, S. C. Dyschromatosis universalis hereditaria: An electron microscopic examination. *J. Dermatol.* **24,** 161–164 (1997).
48. Chin, Y. Y., Chen, G. S., Hu, S. C. S. & Lan, C. C. E. Dyschromatosis universalis hereditaria: A familial case with ultrastructural skin investigation. *Dermatologica Sin.* (2011). doi:10.1016/j.dsi.2011.09.006
49. Delevoye, C. *et al.* AP-1 and KIF13A coordinate endosomal sorting and positioning during melanosome biogenesis. *J Cell Biol* **187,** 247–264 (2009).
50. Cicero, A. Lo *et al.* Exosomes released by keratinocytes modulate melanocyte pigmentation. *Nat. Commun.* **6,** 7506 (2015).
51. Szakacs, G. *et al.* Predicting drug sensitivity and resistance: profiling ABC transporter genes in cancer cells. *Cancer Cell* **6,** 129–137 (2004).
52. Chen, K. G. *et al.* Melanosomal sequestration of cytotoxic drugs contributes to the intractability of malignant melanomas. **103,** 9903–9907 (2006).
53. Basrur, V. Proteomic analysis of early melanosomes: identification of novel melanosomal proteins. *J. Proteome Res.* **2,** 69–79 (2003).
54. Ulrich, D. L. *et al.* ATP-dependent mitochondrial porphyrin importer ABCB6 protects against phenylhydrazine toxicity. *J. Biol. Chem.* (2012). doi:10.1074/jbc.M111.336180
55. Sarkadi, B. *et al.* Human multidrug resistance ABCB and ABCG transporters: participation in a chemoimmunity defense system. *Physiol. Rev.* **86,** 1179–1236 (2006).
56. Slominski, A. *et al.* Hair follicle pigmentation. **124,** 13–21 (2005).
57. Lopes, V. S., Wasmeier, C., Seabra, M. C. & Futter, C. E. Melanosome maturation defect in Rab38-deficient retinal pigment epithelium results in instability of immature melanosomes during transient melanogenesis. *Mol Biol Cell* **18,** 3914–3927 (2007).
58. Barsony, O. *et al.* A single active catalytic site is sufficient to promote transport in P-glycoprotein. *Sci. Rep.* **6,** (2016).
59. Gyimesi, G. *et al.* ABCMdb: A database for the comparative analysis of protein mutations in ABC transporters, and a potential framework for a general application. *Hum. Mutat.* **33,** 1547–1556 (2012).
60. Krishnamurthy, P. C. *et al.* Identification of a mammalian mitochondrial porphyrin transporter. *Nature* **443,** 586–589 (2006).
61. Hurbain, I. *et al.* Melanosome distribution in keratinocytes in different skin types: melanosome clusters are not degradative organelles. *J. Invest. Dermatol.* (2017). doi:10.1016/j.jid.2017.09.039

62. Correia, M. S. *et al.* Melanin transferred to keratinocytes resides in non-degradative endocytic compartments. *J. Invest. Dermatol.* (2017). doi:10.1016/j.jid.2017.09.042
63. Murase, D. *et al.* Autophagy has a significant role in determining skin color by regulating melanosome degradation in keratinocytes. *J. Invest. Dermatol.* **133,** 2416–2424 (2013).
64. Bolte, S. & Cordelières, F. P. A guided tour into subcellular colocalization analysis in light microscopy. *Journal of Microscopy* **224,** 213–232 (2006).
65. Reid, M. E. *et al.* Alleles of the LAN blood group system: Molecular and serologic investigations. *Transfusion* **54,** 398–404 (2014).
66. Shee Hee, J., Mitchell, S. M., Liu, X. & Leonhardt, R. M. Melanosomal formation of PMEL core amyloid is driven by aromatic residues PMEL is a pigment cell protein that forms physiological amyloid in melanosomes. Many amyloids and/ or their oligomeric precursors are toxic, causing or contributing to severe, incurable diseases including Alzheimer's and prion diseases. Striking similarities in intracellular formation pathways between PMEL and various pathological amyloids including Aβ and PrP. *Nat. Publ. Gr.* (2017). doi:10.1038/srep44064
67. Seiji, M., Fitzpatrick, T. B., Simpson, R. T. & Birbeck, M. S. Chemical composition and terminology of specialized organelles (melanosomes and melanin granules) in mammalian melanocytes. *Nature* **197,** 1082–1084 (1963).

Materials and methods

Cell lines, culture conditions and siRNA transfections

MNT1 cells were grown in DMEM high glucose medium (4.5 mg/ml Gibco, Grand Island, NY, USA)) supplemented with 10% v/v AIM-V, 20% v/v FBS, 1% v/v sodium pyruvate, 1% v/v non-essential amino acids, 100 U/ml penicillin and 100 µg/ml streptomycin. MNT1 cells were incubated at 37 °C with 5% CO_2 and regularly passaged at a density of 80% (1:8 ratio). Cells were transfected according to manufacturer's recommendation with siRNA using oligofectamine (Invitrogen). siRNA transfections were performed twice at 48h interval and experiments were performed 96h after the first siRNA transfection. Predesigned siRNAobtained from Qiagen. siRNA non-targeting control: 5'- AAT TCT CCG AAC GTG TCA CGT -3', siRNA ABCB6#1 (Cat no.SI00080353), siRNA ABCB6#2 (Cat no.SI00080360), siRNA ABCB6#3 (Cat no.SI00080374), siRNA ABCB6#4 (Cat

no.SI00083731), siRNA ABCB6#5 (Cat no.SI00080873), siRNA ABCB6#6 (Cat no.SI00080880).

Mutagenesis

Wild type ABCB6 (NM_005689) was mutated by mutagenic PCR to generate the G579E DUH mutation. Mutagenic primers were the following: forward: gtgaaggaccttcctgaagcagggccccttcgc, reverse: gcgaaggggccctgcttcaggaaggtccttcac.

Expression of ABCB6 variants in MNT-1 cells

ABCB6-HA[13] and its non-functional KM mutant variant (ABCB6-HA KM)[16] were expressed in MNT1 cells using lentiviral (LV) transduction. All plasmids used in the production of LV were obtained via the Addgene Plasmid Repository. To produce recombinant lentiviral particles, HEK 293 T human embryonic kidney cells (1.8×10^6 cells on a Petri dish in DMEM–high glucose supplemented with L-glutamine, Penicillin streptomycin, and 10% FBS) were transfected with (6 μg) pSEW-EF1-ABCB6-PGK-Puromycine expression plasmid, 2.2 μg pMD2.G envelope- and 4 μg psPax2 second-generation packaging plasmids, using the $CaPO_4$ precipitation transfection method. Conditioned medium, containing lentiviral particles, was collected 72 h after transfection. The supernatant was cleared by filtration through 0.45-μm PVDF membrane filters (Millipore), snap frozen, and stored at −80 °C until further use. Transduction of target MNT1 cells was carried out on 6 well plates. The multiplicity of infection was approximately 1.

Lysates, cell fractionation and Western blot:

For Western blots a Triton X-soluble lysate was prepared in 20 mM Tris-HCl pH 7.4, 150 mM NaCl, 1% TX-100, 1 mM EDTA, protease inhibitors. The Triton X-insoluble fraction was resuspended in 1% SDS, 1% B-mercaptoethanol in PBS containing protease inhibitors, incubated for 10 min at RT and then heated for 10 min at 100°C. Light and dense melanosomal fractions and exosome isolation were performed as already described[25,36]. Lysates, fractions and exosomes were incubated in sample buffer with or without 350 mM 2-mercapthethanol (Sigma), incubated at 60°C for 5 min, and fractionated by SDS-PAGE using Nupage (4-12%) Bis-Tris gels (Invitrogen) and transferred onto nitrocellulose membranes (Millipore). The membranes were blocked in PBS/Tween 0.1% (PBS/T) with 5% non-fat dried milk, incubated with the indicated primary antibody diluted in PBS/T, washed four times in blocking solution, and finally incubated with HRP-conjugated secondary antibody followed by washing in PBS/T.

Blots were developed using the ECL Plus Western blotting detection system (GE Healthcare) according to the manufacturer's instruction. Signal intensities were quantified with the Image J software (National Institute of Health).

Melanin assay

Cells were disrupted by sonication in 50 mM Tris-HCl, pH 7.4, 2 mM EDTA, 150 mM NaCl, 1 mM DTT, and protease inhibitors. Pigment was pelleted at 16000g for 15min at 4°C, rinsed once in ethanol/ether (1:1), and dissolved in 2M NaOH/20% DMSO at 60°C. Melanin content was measured as optical density at 492nm.

Immunofluorescence Microscopy. MNT-1 cells expressing ABCB6 variants were plated in Eppendorf 8 well imaging coverglass (#0030742036). Hoechst 33342 was applied to the cells 20 min prior to fixation, subsequently cells were rinsed in PBS and fixed for 30 min in 4% Paraformaldehyde/PBS at room temperature (RT). Fixed cells were quenched for 10min in PBS/100mM glycine (quenching buffer), washed with PBS and blocked and permeabilized in PBS containing 0.2 mg/ml BSA/0.1% Triton X-100/ 10% Normal Goat Serum (blocking buffer). Primary antibody was diluted in PBS containing 0.2mg/ml BSA/0.1%Triton X-100/3% Normal Goat Serum (incubation buffer, IB). Cells were incubated with the primary antibody overnight at 4°C in a humidified chamber, washed five times in IB, and incubated with the corresponding secondary anti-human, anti-rabbit and anti-mouse antibodies conjugated to Alexa Fluor 488 or Alexa Fluor 647 diluted in IB for 90 min at RT. Samples were washed five times with PBS and subsequently imaged. Confocal images were obtained using a LSM 880 confocal laser scanning microscope (Carl Zeiss, Inc.) equipped with a Plan-Apochromat 63×/1.4 NAOil DIC M27objective. Images were acquired in three channels (blue [Hoechst33342], green [Alexa Fluor 488], red [Alexa Fluor 647], blue emitting Hoechst 33342 was excited using the 405nm laser line, green emitting Alexa Fluor 488 was excited using the 488nm laser line and infrared emitting Alexa Fluor 647 was excited using the 633nm laser line. Noise reduction and deconvolution of the images was performed with Huygens Essential (Scientific Volume Imaging B.V.). Colocalization analysis was performed with ImageJ (National Institute of Health) using the JACoP v2.0 plugin.[64]

Antibodies and Dyes.

Monoclonal antibodies and their sources were as follows: Mouse monoclonal Anti-Melanoma Associated Antigen 100+/7 kDa [Nki/beteb] antibody (ab34165; used for IFM and EM) and

mouse monoclonal Anti-Melanoma [HMB45] antibody (ab787; used for IFM and EM) to melanocyte protein (PMEL), mouse monoclonal Anti-TRP-1 [TA99] antibody (ab3312; used for IFM and EM) to tyrosinase-related protein 1(TRP1), secondary goat polyclonal antibody to human IgG conjugated to DyLight 488 (ab96907) and horseradish peroxidase-conjugated goat polyclonal antibodies to rabbit IgG (ab6721) and to mouse IgG (ab6789) were from Abcam. Rabbit monoclonal Anti-AIF [D39D2] antibody (#5318) to apoptosis inducing factor, rabbit monoclonal Anti-Calnexin [C5C9] antibody (#2679) to Calnexin, rabbit monoclonal Anti-RCAS1 [D2B6N] to receptor binding cancer antigen expressed on SiSo cells (#12290), rabbit monoclonal Anti-EEA1 [C45B10] antibody (#3288) to early endosome antigen 1, rabbit monoclonal Anti-LAMP1 [D2D11] antibody (#9091) to lysosome-associated membrane protein 1, secondary goat anti-mouse IgG (H+L) $F(ab')_2$ fragment conjugated to Alexa Fluor 647 (#4410) and secondary goat anti-rabbit IgG (H+L) $F(ab')_2$ fragment conjugated to Alexa Fluor 647 (#4414) were from Cell Signaling Technology. Secondary goat anti-rabbit IgG (H+L) antibody conjugated to Alexa Fluor-488 (A-11034) and Hoechst 33342 (R37605) nuclear counterstain were from Thermo Fisher Scientific. The OSK43 antibody was a kind gift from Dr Yoshihiko Tani (Japanese Red Cross Osaka Blood Center, Osaka,Japan)[65]. ABCB6 ((61.5): sc-135726) mouse monoclonal antibody was from Santa Cruz Biotechnology. Affinity-purified anti-peptide antibodies recognizing the PMEL N-terminus (**α**-PMEL-Nter)[21], C-terminus (**α**-PMEL-Cter) [20] and PKD domain (I51 - kind gift from P. Cresswell, N. Vigneron, and R. M. Leonhardt, Yale Univ., New Haven, CT)[66] were used as described previously. Mouse anti-CD63 used for IEM was from Zymed/Invitrogen. Protein A conjugated to 10- or 15-nm gold particles (PAG10, PAG15) were from Cell Microscopy Center (Utrecht University Hospital, Utrecht University, Utrecht, The Netherlands).

Animal experiments

Abcb6 -/+ mice were obtained from The Jackson Laboratory following in vitro fertilization of C57BL/6J female mice by cryopreserved Abcb6 $^{-/-}$ sperm. Heterozygous and homozygous mice were generated by intercrossing F1 heterozygous mice. Genotyping of the mice was performed with the following primers: 5'- GGCTGAGGATAGACTAGGCTCTG- 3'; 5'- CCTGTGTGTTCATATCACGGCG- 3'; and 5'- CTGCCTTGGGAA AAGCGCCTC- 3'.

Mice were housed in SPF animal house in cages with free access to water and ad libitum diet. All animal procedures were performed in accordance with the EU's most recent directives, as approved by the Committee on the Care and Use of Laboratory Animals of the Council on Animal Care at the Institute of Enzymology, RCNS in Budapest, Hungary. For the preparation

of electron microscopy samples, 6 months old female mice were sacrificed; enucleated eyes were immediately fixed in Glutaraldehyde solution (Sigma).

Electron microscopy

For conventional EM on resin embedded cells, MNT-1 were grown on coverslips, fixed in 2.5% glutaraldehyde in 0.1 M cacodylate buffer for 24 h, post-fixed with 1% osmium tetroxide, dehydrated in ethanol and embedded in epon as described[20]. For EM analysis of RPE sections, tissues from mice were processed as previsouly[22], ultrathin sections of RPE were prepared with a Reichert UltracutS ultramicrotome (Leica Microsystems) and contrasted with uranyl acetate and lead citrate. For ultrathin cryosectioning and immunogold labeling, cells were fixed in 2% PFA, 0.2% glutaraldehyde in 0.1M phosphate buffer pH 7.4. Cells were processed for ultracryomicrotomy and immunogold labeled using PAG 10 and PAG 15 as described[20]. All samples were examined with a FEI Tecnai Spirit electron microscope (FEI Company), and digital acquisitions were made with a numeric camera (Quemesa; Soft Imaging System). Melanosome stages were defined by morphology[20,67]. Length and width of melanosomes, as well as the size were measured using ImageJ software. P values were determined by Student's t-test, unpaired, unequal variance (*$p<0.05$, **$p<0.01$, ***$p<0.001$).

Figure 1

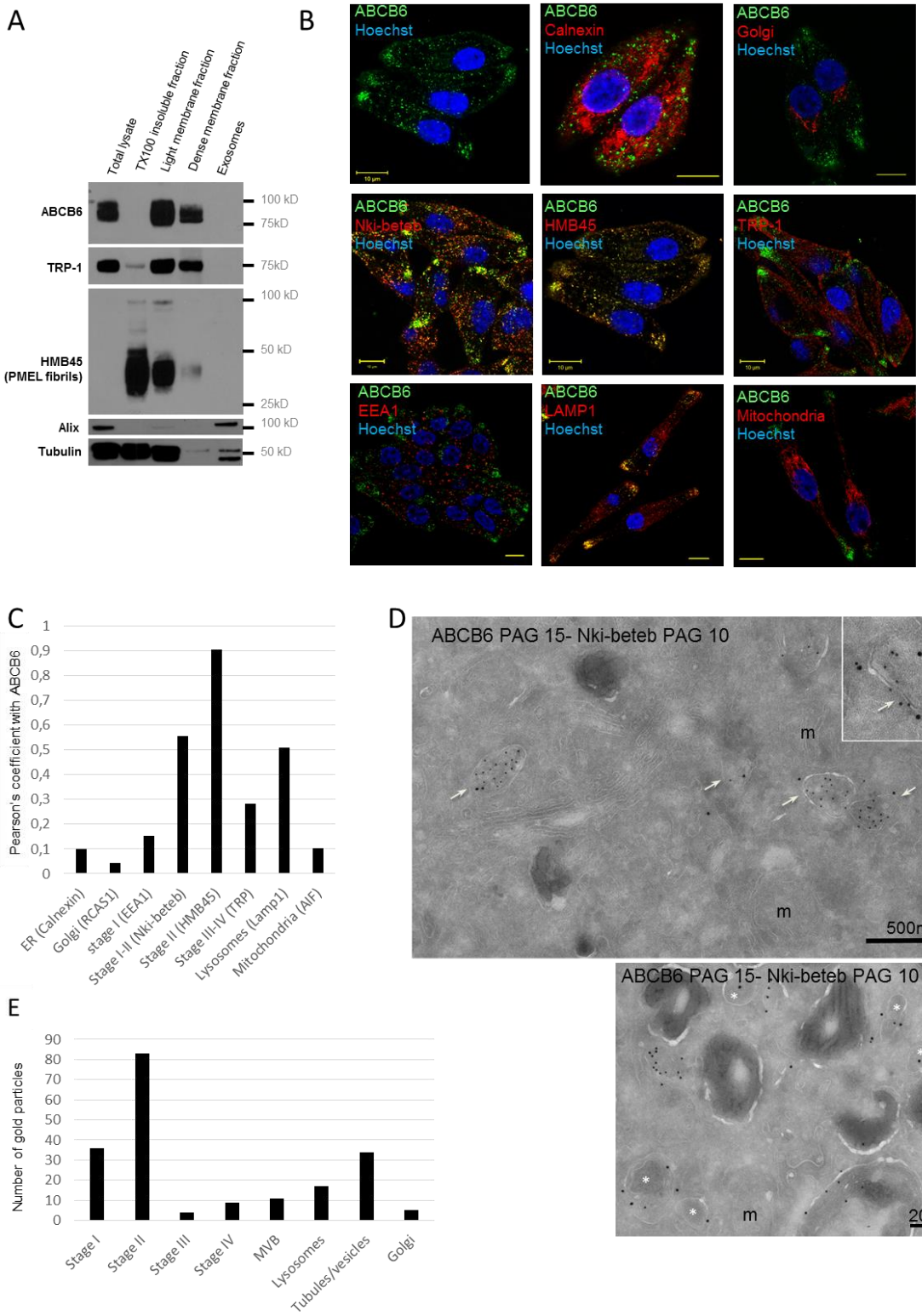
A
Total lysate
TX100 insoluble fraction
Light membrane fraction
Dense membrane fraction
Exosomes
ABCB6
TRP-1
HMB45 (PMEL fibrils)
Alix
Tubulin
100 kD
75kD
75kD
100 kD
50 kD
25kD
100 kD
50 kD
B
ABCB6 Hoechst
ABCB6 Calnexin Hoechst
ABCB6 Golgi Hoechst
ABCB6 Nki-beteb Hoechst
ABCB6 HMB45 Hoechst
ABCB6 TRP-1 Hoechst
ABCB6 EEA1 Hoechst
ABCB6 LAMP1 Hoechst
ABCB6 Mitochondria Hoechst
C
Pearson's coefficient with ABCB6
1
0,9
0,8
0,7
0,6
0,5
0,4
0,3
0,2
0,1
0
ER (Calnexin)
Golgi (RCAS1)
stage I (EEA1)
Stage I-II (Nki-beteb)
Stage II (HMB45)
Stage III-IV (TRP)
Lysosomes (Lamp1)
Mitochondria (AIF)
D
ABCB6 PAG 15- Nki-beteb PAG 10
m
m
500nm
ABCB6 PAG 15- Nki-beteb PAG 10
m
200nm
E
Number of gold particles
90
80
70
60
50
40
30
20
10
0
Stage I
Stage II
Stage III
Stage IV
MVB
Lysosomes
Tubules/vesicles
Golgi

Figure 2

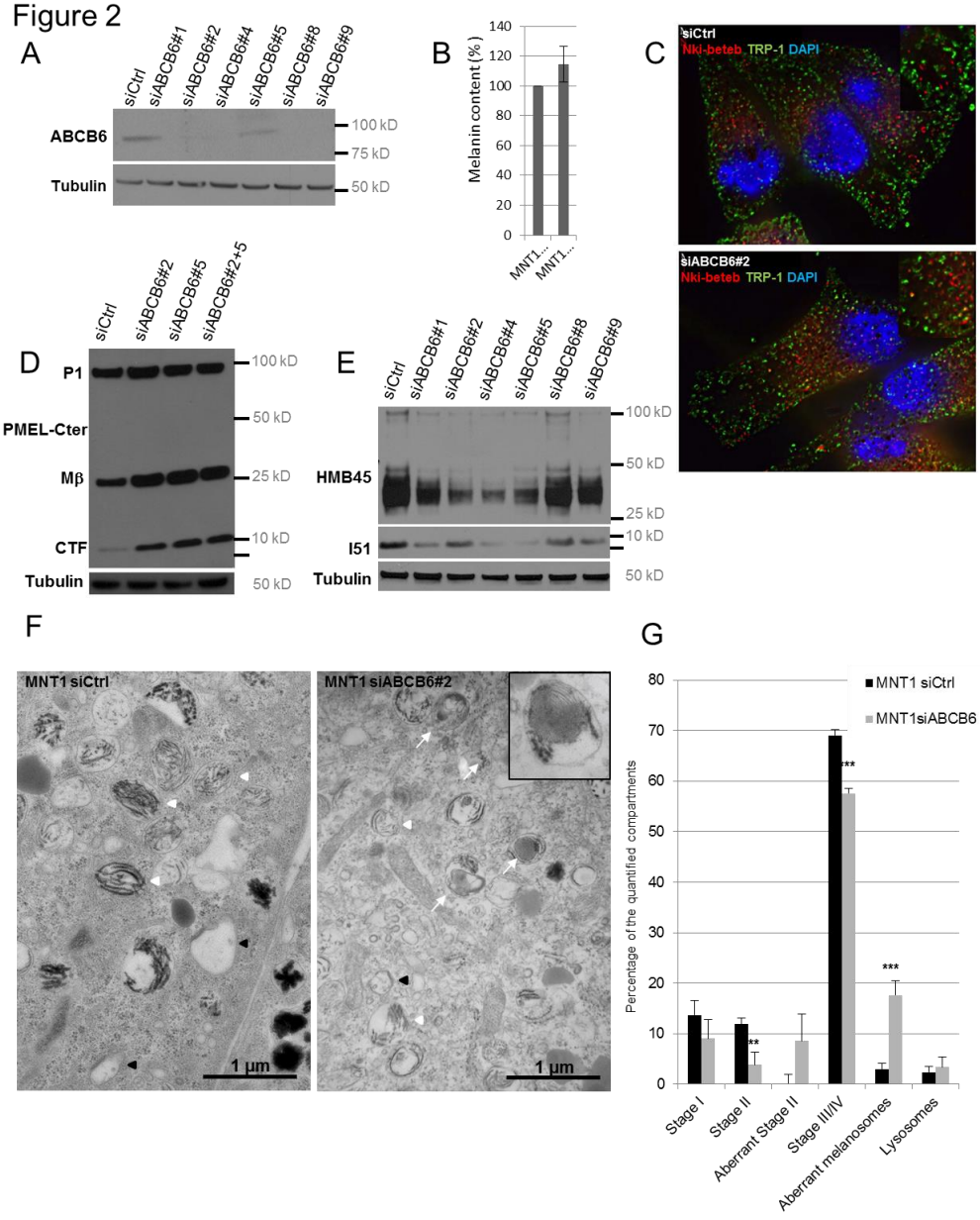
A
siCtrl
siABCB6#1
siABCB6#2
siABCB6#4
siABCB6#5
siABCB6#8
siABCB6#9
ABCB6
Tubulin
100 kD
75 kD
50 kD
B
Melanin content (%)
140
120
100
80
60
40
20
0
MNT1...
MNT1...
C
siCtrl
Nki-beteb TRP-1 DAPI
siABCB6#2
Nki-beteb TRP-1 DAPI
D
siCtrl
siABCB6#2
siABCB6#5
siABCB6#2+5
P1
PMEL-Cter
Mβ
CTF
Tubulin
100 kD
50 kD
25 kD
10 kD
50 kD
E
siCtrl
siABCB6#1
siABCB6#2
siABCB6#4
siABCB6#5
siABCB6#8
siABCB6#9
HMB45
I51
Tubulin
100 kD
50 kD
25 kD
10 kD
50 kD
F
MNT1 siCtrl
MNT1 siABCB6#2
1 µm
1 µm
G
MNT1 siCtrl
MNT1siABCB6
Percentage of the quantified compartments
80
70
60
50
40
30
20
10
0
**
***
***
Stage I
Stage II
Aberrant Stage II
Stage III/IV
Aberrant melanosomes
Lysosomes

A

Figure 3

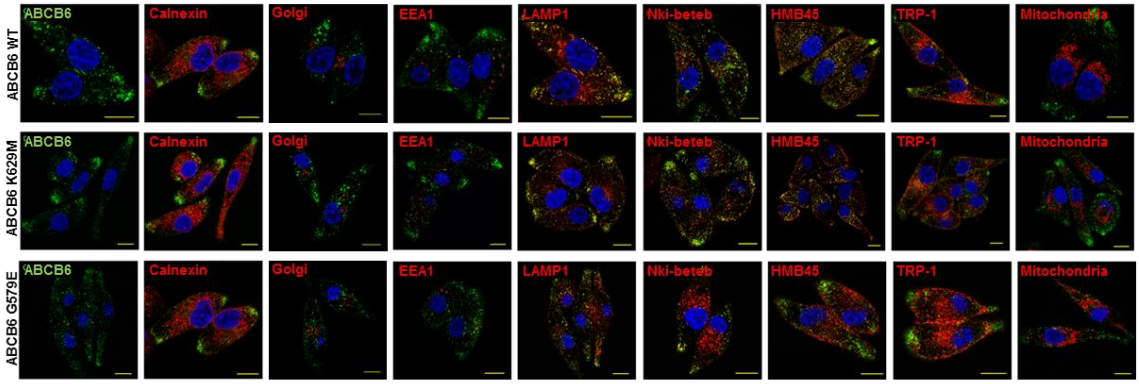

B

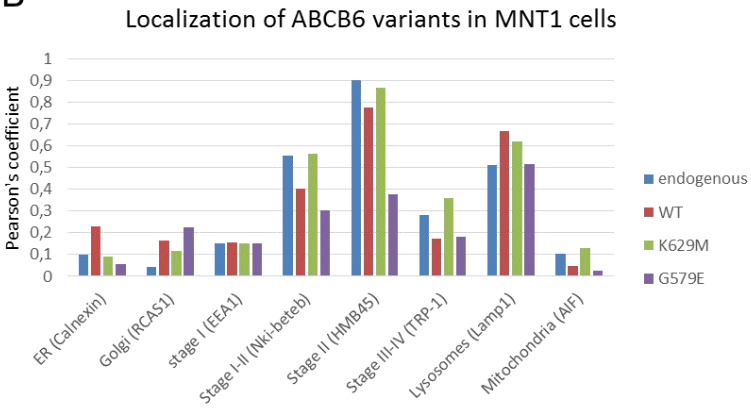

C

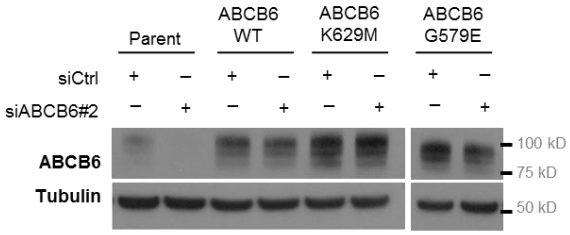

D

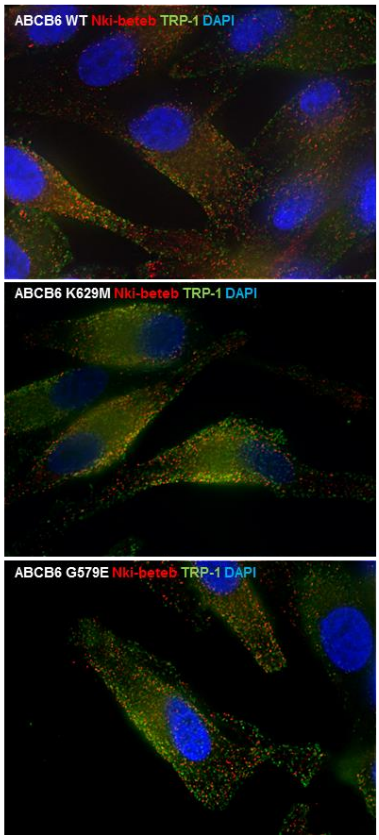

Figure 4

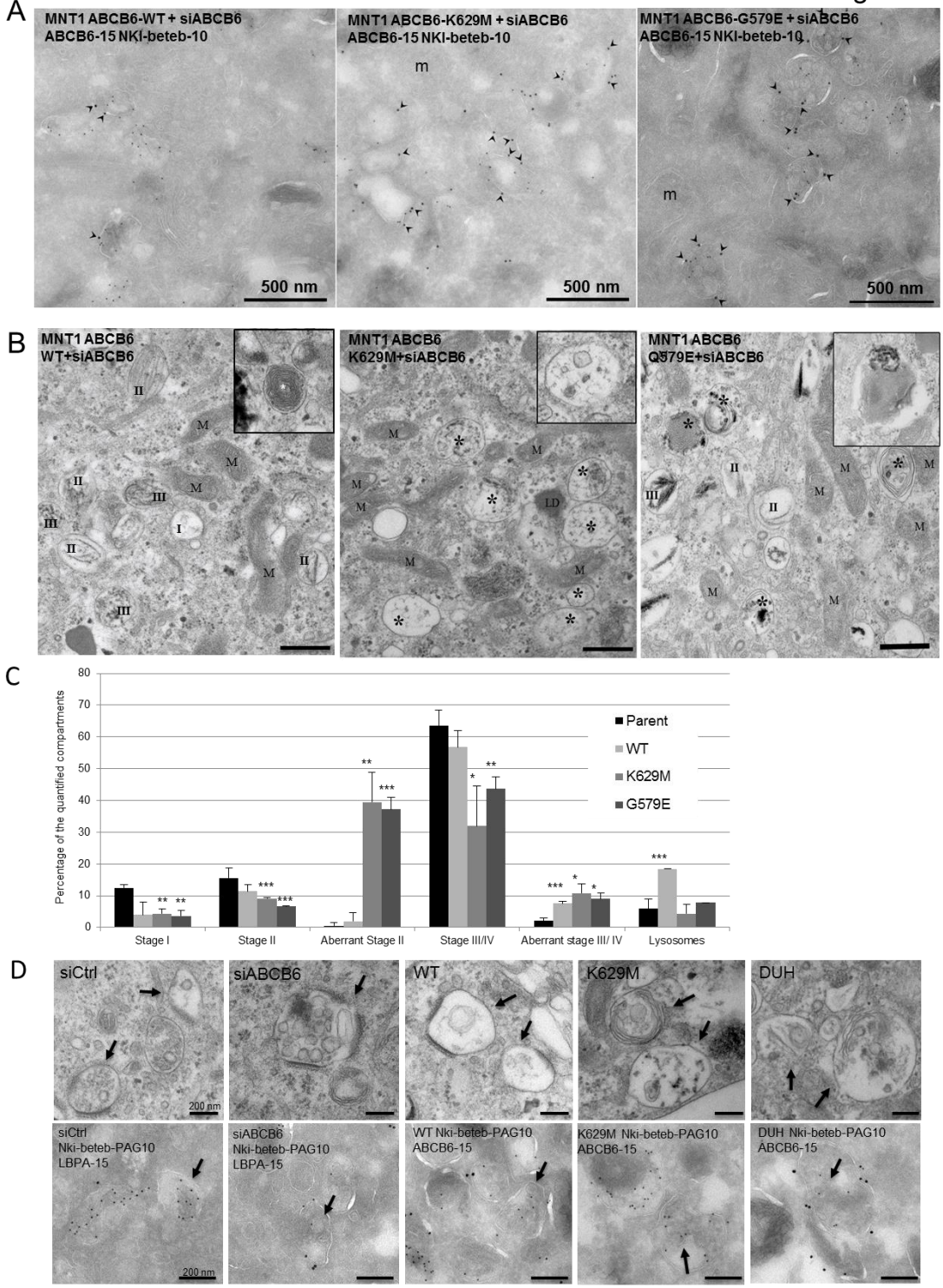
A
MNT1 ABCB6-WT + siABCB6
ABCB6-15 NKI-beteb-10
MNT1 ABCB6-K629M + siABCB6
ABCB6-15 NKI-beteb-10
MNT1 ABCB6-G579E + siABCB6
ABCB6-15 NKI-beteb-10
500 nm
B
MNT1 ABCB6
WT+siABCB6
MNT1 ABCB6
K629M+siABCB6
MNT1 ABCB6
Q579E+siABCB6
C
Percentage of the quantified compartments
Parent
WT
K629M
G579E
Stage I
Stage II
Aberrant Stage II
Stage III/IV
Aberrant stage III/ IV
Lysosomes
D
siCtrl
siABCB6
WT
K629M
DUH
200 nm
siCtrl
Nki-beteb-PAG10
LBPA-15
siABCB6
Nki-beteb-PAG10
LBPA-15
WT Nki-beteb-PAG10
ABCB6-15
K629M Nki-beteb-PAG10
ABCB6-15
DUH Nki-beteb-PAG10
ABCB6-15

Figure 5

A

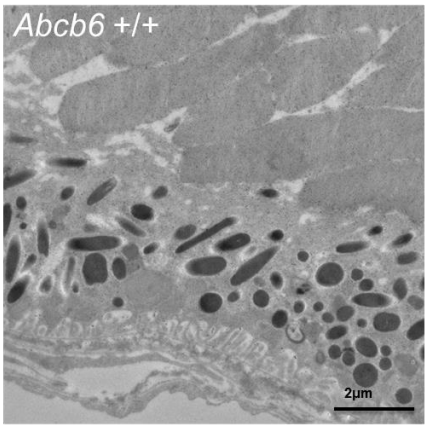
Abcb6 +/+
2µm

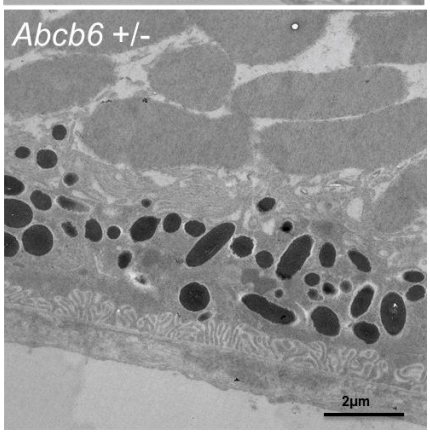
Abcb6 +/-
2µm

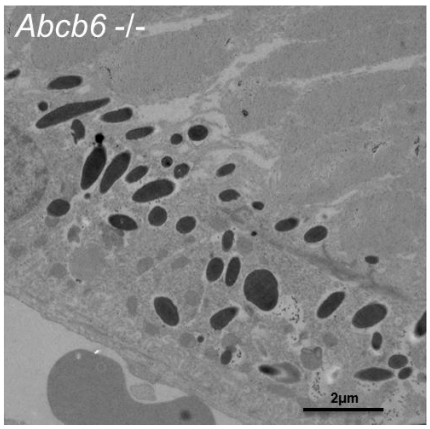
Abcb6 -/-
2µm

B

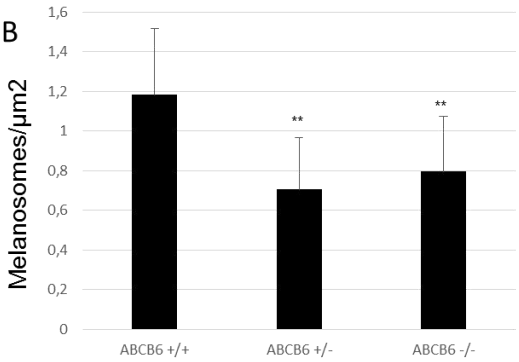
Melanosomes/µm2
1,6
1,4
1,2
1
0,8
0,6
0,4
0,2
0
**
**
ABCB6 +/+
ABCB6 +/-
ABCB6 -/-

C

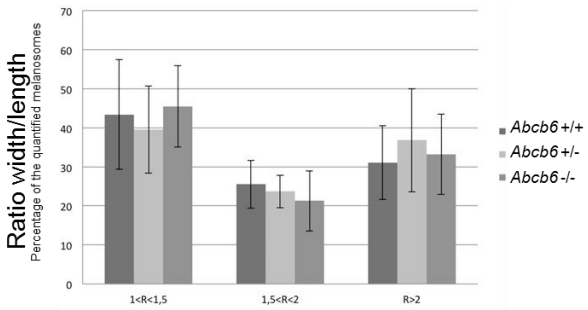
Ratio width/length
Percentage of the quantified melanosomes
70
60
50
40
30
20
10
0
1<R<1,5
1,5<R<2
R>2
Abcb6+/+
Abcb6+/-
Abcb6-/-